

Conformation of Hexahydroxycalix[6]arene

Willem P. van Hoorn, Frank C. J. M. van Veggel, and
David N. Reinhoudt*

Laboratory of Organic Chemistry, University of Twente,
P.O. Box 217, 7500 AE Enschede, The Netherlands

Received May 13, 1996

Introduction

Calix[*n*]arenes (*n* = 4–8), cyclic oligomeric condensates of phenols and formaldehyde, are frequently used as building block in supramolecular chemistry.¹ The conformation of *p*-*tert*-butylhexahydroxycalix[6]arene (**1**) (Chart 1) in the solid state^{2,3} is called a *pinched cone* because two methylene bridges are pointing into the cavity (Figure 1a).

Intramolecular hydrogen bond formation determines the stability of conformations of unsubstituted calix[*n*]arenes.^{4,5} The skeleton of **1** is pinched to allow for a circular array of six hydrogen bonds. Early measurements by Gutsche *et al.* with ¹H NMR spectroscopy have shown that in solution calix[6]arene **1** is conformationally flexible. From the coalescence of the methylene hydrogens, they postulated the interconversion of two equivalent cone conformations. The free energy barrier ΔG^\ddagger of the inversion process in different solvents is in the range of 11–13 kcal mol⁻¹.⁴ Recently, Molins *et al.*⁶ published a sophisticated 2D NMR study of upper rim substituted trichlorocalix[6]arene **2**. They calculated a 3D conformation of **2** by performing a molecular dynamics simulation with constraints for the hydroxy–hydroxy and hydroxy–methylene distances determined by NMR. Their conformation is described as a *winged cone*, with four aryl groups in up alignment and two aryl groups located at opposite sites bent outside (Figure 1b). All six methylene bridges are pointing outward. They reported that the conformation is stabilized by a cyclic array of six hydrogen bonds.⁶ This conformation exhibits three different dynamic processes: macrocyclic ring inversion, pseudorotation, and hydrogen bond reversal.

The findings of Molins *et al.* have recently been disputed by our group.⁷ We claimed that the *pinched cone* found in the solid state^{2,3} is also the conformation in solution and that the processes of pseudorotation and macrocyclic ring inversion are *one* concerted pseudorotation/inversion process. In this Note we will support our reinterpretation of the NMR experiments of Molins *et al.*

(1) (a) Gutsche, C. D. *Calixarenes*; Royal Society of Chemistry; Cambridge, 1989. (b) *Calixarenes. A Versatile Class of Compounds*; Vicens, J., Böhmer, V., Eds.; Kluwer Academic Publishers: Dordrecht, The Netherlands, 1991.

(2) Andreetti, G. D.; Ugozzoli, F.; Casnati, A.; Ghidini, E.; Pochini, A.; Ungaro, R. *Gazz. Chim. Ital.* **1989**, *119*, 47.

(3) Halit, M.; Oehler, D.; Perrin, M.; Thozet, A.; Perrin, R.; Vicens, J.; Bourakhoudar, M. *J. Inclusion Phenom.* **1988**, *6*, 613.

(4) Gutsche, C. D.; Bauer, J. *J. Am. Chem. Soc.* **1985**, *107*, 6052.

(5) (a) Lutz, B. T. G.; Astarloa, G.; van der Maas, J. H.; Janssen, R. G.; Verboom, W.; Reinhoudt, D. N. *Vib. Spectrosc.* **1995**, *10*, 29. (b) Janssen, R. G.; Verboom, W.; Lutz, B. T. G.; van der Maas, J. H.; Maczka, M.; van Duynhoven, J. P. M.; Reinhoudt, D. N. *J. Chem. Soc., Perkin Trans. 2* **1996**, in press.

(6) Molins, M. A.; Nieto, P. M.; Sánchez, C.; Prados, P.; de Mendoza, J.; Pons, M. *J. Org. Chem.* **1992**, *57*, 6924.

(7) Janssen, R. G.; van Duynhoven, J. P. M.; Verboom, W.; van Hunmel, G. J.; Harkema, S.; Reinhoudt, D. N. *J. Am. Chem. Soc.* **1996**, *118*, 3666.

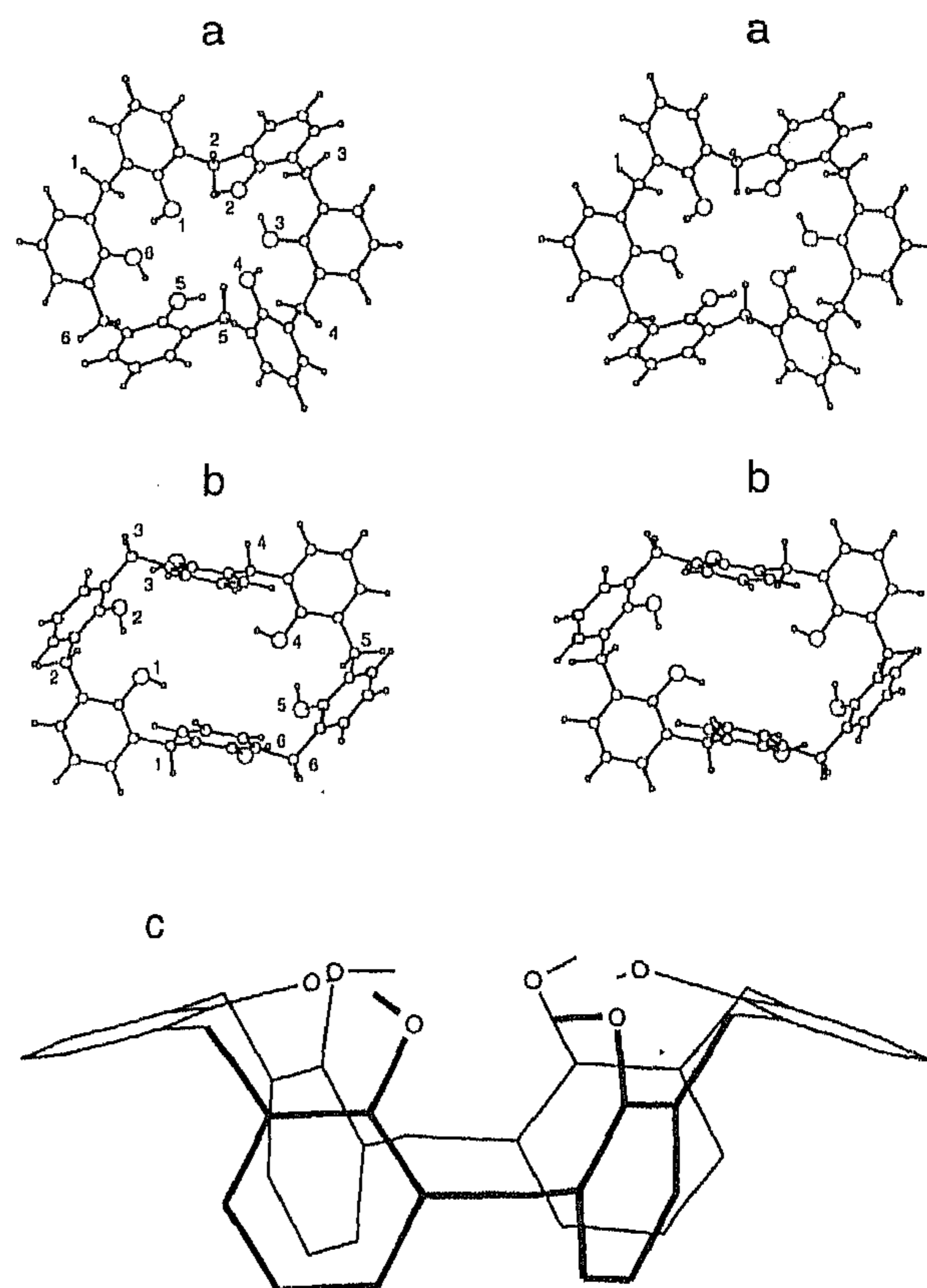
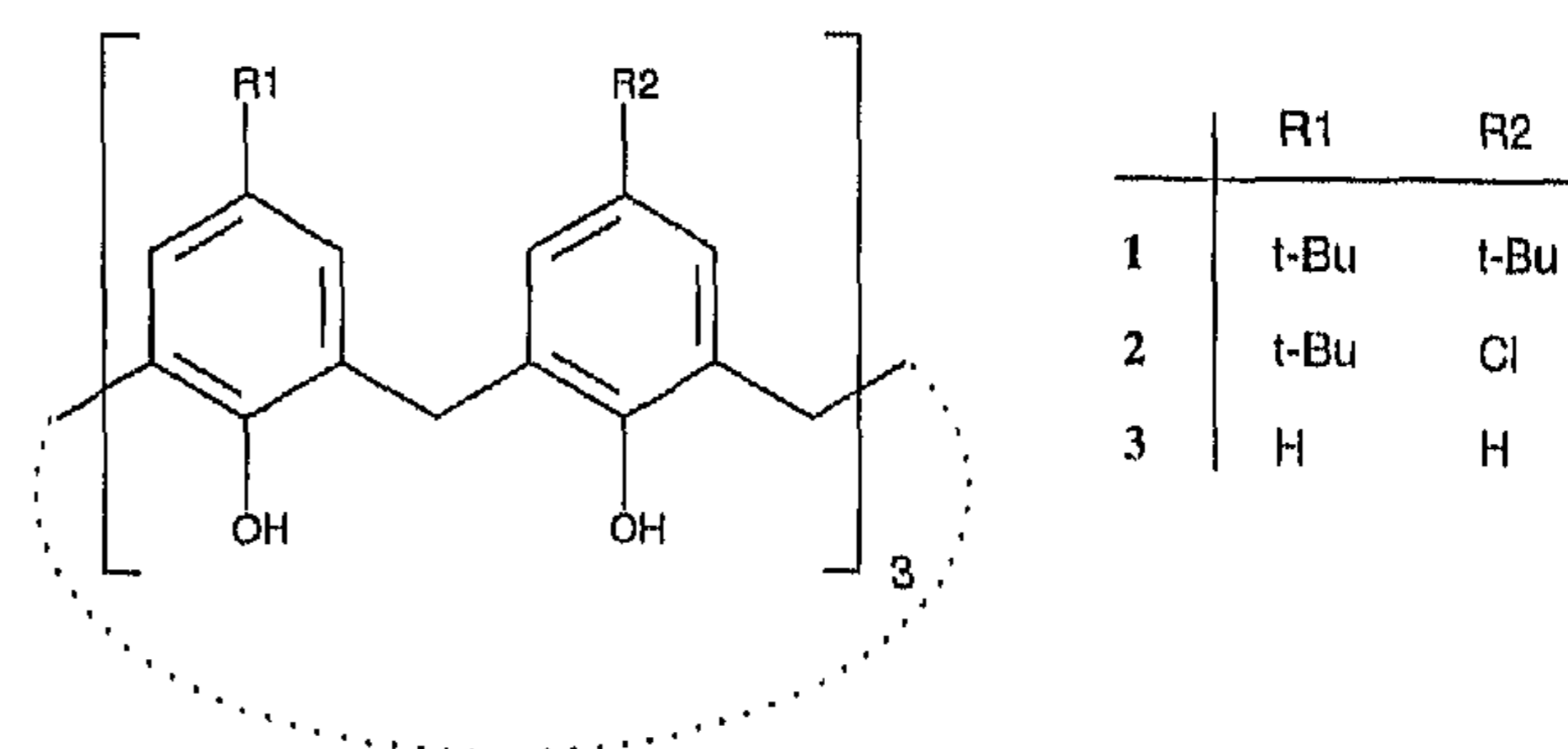


Figure 1. Energy-minimized *pinched* (a) and *winged* (b) cone conformations of **3**. The *pinched cone* is built from the X-ray determined conformation of **1**.² The *winged cone* is proposed by Molins *et al.* for **2** in dichloromethane solution.⁶ The side view of the *winged cone* (c) is to be compared with Figure 6 in ref 6.

Chart 1



using molecular modeling.^{8,9,10} We will show that the measured energy barriers and proton–proton distances can be explained assuming a *pinched cone* in solution and that this conformation is the most stable.

Methods

Energy Minimization. Version 23f3 of the CHARMM¹¹ program was used. Energies of the calix[4]arenes were evaluated with the parameters, partial charges, and energy function described in ref 9. The energies of the conformations were minimized until the root mean square value of the energy

(8) Grant, G. H.; Richards, W. G. *Computational Chemistry*; Oxford University Press: Oxford, 1995.

(9) Fischer, S.; Grootenhuis, P. D. J.; Groenen, L. C.; van Hoorn, W. P.; van Veggel, F. C. J. M.; Reinhoudt, D. N.; Karplus, M. *J. Am. Chem. Soc.* **1995**, *117*, 1611.

(10) van Hoorn, W. P.; Briels, W. J.; van Duynhoven, J. P. M.; van Veggel, F. C. J. M.; Reinhoudt, D. N. Submitted for publication.

(11) Brooks, B. R.; Brucoleri, R. E.; Olafson, B. D.; States, D. J.; Swaminathan, S.; Karplus, M. *J. Comput. Chem.* **1983**, *4*, 187.

gradient was less than 10^{-12} kcal mol $^{-1}$ Å $^{-1}$. The *pinched* cone of unsubstituted calix[6]arene **3** was constructed from the conformation published by Andreotti *et al.*² The *winged* cone of **3** was constructed by energy minimization of a cone with all methylene bridges pointing outward. Inverted conformations were generated by multiplying the *z*-coordinate of all atoms by -1 . Pseudorotated conformations were generated by reordering the residue numbers from 123456 to 612345. Quanta4.0¹² was used to build conformations and generate molecular graphics.

TRAVEL. The conjugate peak refinement (CPR) algorithm^{9,13,14} searches for maxima along the adiabatic energy valley connecting two local minima on the potential energy surface. These maxima are subsequently refined to saddle points and represent the transition states of the reaction pathway between the two minima. All the degrees of freedom of the molecule can contribute to the reaction path. There is no need to choose a reduced reaction coordinate such as a rotation around a certain bond. In the course of the path refinement, the CPR algorithm generates intermediates by linear interpolation in Cartesian coordinates of the minima. Intermediate conformations can also be provided to the CPR algorithm as initial guess in order to improve converge or to force a certain pathway. The output consists of a series of *N* intermediates (each given by its coordinate vector \mathbf{r}_i) along the reaction coordinate from the reactant \mathbf{r}_0 to the product \mathbf{r}_{N+1} , including one or more saddle points. The one-dimensional reaction coordinate λ is given by

$$\lambda_i = \sum_{j=0}^{i-1} |\mathbf{r}_{j+1} - \mathbf{r}_j|$$

The algorithm has been integrated into CHARMM¹¹ in the TRAVEL module. The calculated pathways were smoothed with the synchronous chain minimization algorithm.^{15,16}

Results and Discussion

Energy Minimization. The para substituents R1 and R2 (Chart 1) have only a minor influence on the measured energy barriers.^{4,6} Therefore, all calculations have been performed on unsubstituted calix[6]arene **3**. The key difference between the *pinched* and *winged* cone conformations is the orientation of the methylene bridges. For the *winged* cone, all methylene bridges are pointing out of the cavity. For the *pinched* cone, two diametrical methylene bridges are pointing into the cavity. The *pinched* cone of **3** is believed to be optimal for the intramolecular hydrogen bonds as determined with IR spectroscopy.^{5,17} In the CHARMM force field the energy of hydrogen bonds is represented within the electrostatic energy. After minimizing the potential energy, we find that the *pinched* cone has a 13.8 kcal mol $^{-1}$ more favorable electrostatic energy than the *winged* cone (Table 1). The total potential energy of the *pinched* cone is 16.2 kcal mol $^{-1}$ more favorable. This result shows that the *pinched* cone is by far favored over the *winged* cone and that this is mainly due to the more optimal hydrogen bond geometry of the *pinched* cone. In the *winged* cone, two OH...O distances are too long (4.1 Å) for a hydrogen bond.¹⁸ Therefore, the *winged* cone does not contain one circular array of six hydrogen bonds, but two

Table 1. Calculated Energies and Experimental Energy Barriers of **3** (kcal mol $^{-1}$)^a

conformation	<i>pinched</i> cone			<i>winged</i> cone			ΔG^\ddagger
	E_{total}	E_{dihedral}	E_{elec}	E_{total}	E_{dihedral}	E_{elec}	
minimized cone	0.0	0.0	0.0	16.2	3.1	13.8	
TS _{pseudorotation}	19.4	10.0	14.2	19.3	13.1	11.8	12.2
TS _{inversion}	26.7	-1.2	25.2	29.3	4.1	23.0	12.8
TS _{inversion+pseudorotation}	13.0	-0.4	12.5	29.3	4.1	23.0	

^a All calculated energies are normalized to the energy of the minimized *pinched* cone. The two largest contributions to the total potential energy (E_{total}) are for most conformations the dihedral angle (E_{dihedral}) and electrostatic energies (E_{elec}). ΔG^\ddagger = experimentally determined free energy barriers from ref 6. TS = transition state.

Table 2. Hydroxy-Hydroxy and Hydroxy-Methylene Distances (Å) of **3**^a

res ^b	<i>pinched</i> cone			<i>winged</i> cone		
	CH ^{ax} :OH	CH ^{eq} :OH	OH:OH	CH ^{ax} :OH	CH ^{eq} :OH	OH:OH
2:1	4.7	3.4	2.6	3.7	4.9	2.7
2:2	3.5	2.2		2.0	3.5	
3:2	3.6	4.9	2.6	3.7	4.9	2.6
3:3	2.0	3.5		2.0	3.5	
4:3	3.4	4.8	2.3	3.5	3.8	4.7
4:4	2.2	3.5		1.9	3.4	

^a Due to the C_2 symmetry present in both cone conformations, only half of the distances are presented. ^b Residue numbers in Figure 1.

arrays of two hydrogen bonds, as already predicted by Gutsche on basis of CPK models.⁴

Structural Differences. Both *pinched* and *winged* cones have one C_2 axis perpendicular to the mean plane of the methylene bridges, in accordance with the ^1H NMR spectrum.⁶ Molins *et al.* have constructed the *winged* cone of **2** by constraining the methylene-hydroxy and hydroxy-hydroxy proton distances.⁶ In Table 2 these distances are presented for both the energy-minimized *pinched* and *winged* cones of **3**. Both conformations are virtually indistinguishable when looking at the methylene-hydroxy distances. The largest difference is for the 4:3 (and 1:6) CH^{eq}-OH distance which is 4.8 Å for the *pinched* cone and 3.8 Å for the *winged* cone. For the hydroxy-hydroxy proton distances, there is one clear difference. The 4:3 (and 1:6) OH-OH distance is 2.3 Å for the *pinched* cone and 4.7 Å for the *winged* cone. The ROESY cross peaks between the OH protons of a partially deuterated sample of **2** do not indicate that one pair of OH-OH distances is larger than the others.⁶ Molins *et al.* concluded that the *winged* cone is the most stable conformation in solution, probably because their optimization was trapped in the *winged* cone local energy minimum.^{19,20}

Dynamical Properties. We calculated for both cone conformations of **3** the pathways for pseudorotation and inversion with TRAVEL.^{21,22} Inversion is the rotation of the six aromatic rings with the hydroxy moiety through the cavity. During inversion of either cone conformation, the hydrogen atoms of the six methylene bridges ex-

(12) QUANTA version 4.0; Molecular Simulations Inc., Waltham, MA.

(13) Fischer, S.; Karplus, M. *Chem. Phys. Lett.* **1992**, *194*, 252.

(14) (a) Fischer, S.; Dunbrack, R. L., Jr.; Karplus, M. *J. Am. Chem. Soc.* **1994**, *116*, 11931. (b) Verma, C. S.; Fischer, S.; Caves, L. S. D.; Roberts, G. C. K.; Hubbard, R. E. *J. Phys. Chem.* **1996**, *100*, 2510.

(15) Fischer, S. Manuscript in preparation.

(16) The SCM algorithm does not affect the calculated saddle point(s).

(17) Araki, K.; Iwamoto, K.; Shinkai, S.; Matsuda, T. *Bull. Chem. Soc. Jpn.* **1990**, *63*, 3480.

(18) Jeffrey, G. A.; Saenger, W. *Hydrogen Bonding in Biological Structures*; Springer-Verlag: Berlin, 1991.

(19) Lipkowitz, K. B. *J. Chem. Educ.* **1995**, *72*, 1070.

(20) Only two (the 4:3 and 1:6 OH-OH distances) of the 30 hydroxy-hydroxy and hydroxy-methylene distance constraints are violated in a *winged* cone. The *pinched* and *winged* cone conformations are also indistinguishable when looking at the methylene-aromatic distances.

(21) Hydrogen bond reversal can proceed via proton tunneling or can be catalyzed by traces of water.^{6,22} Both of these mechanisms cannot be modeled adequately by force field calculations and are therefore not dealt with here.

(22) Kim, Y. *J. Am. Chem. Soc.* **1996**, *118*, 1522.

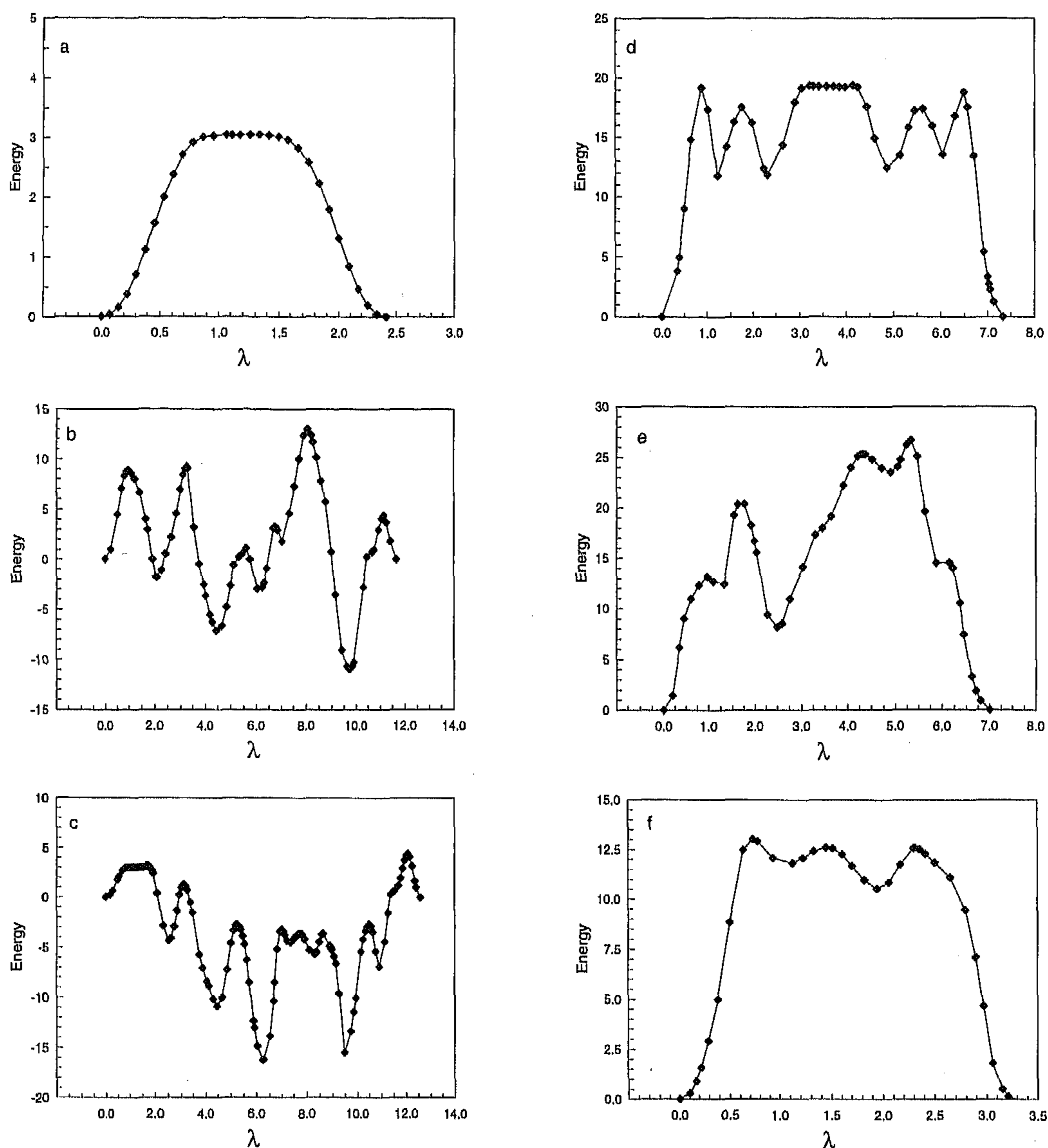


Figure 2. Energy profiles (kcal mol^{-1}) along the reaction coordinate λ (\AA) for dynamic processes of **3**. Depicted are pseudorotation (a), inversion (b), and pseudorotation/inversion (c) of the *winged* cone and pseudorotation (d), inversion (e), and pseudorotation/inversion (f) of the *pinched* cone. The energies are normalized to the energies of the respective minimized cones.

change equatorial and axial positions. During pseudorotation of the *pinched* cone, the two methylene moieties pointing into the annulus exchange to a position pointing outward, two other diametrical methylene bridges undergo the reverse exchange. For the *winged* cone, the two phenol rings in an out position exchange with two phenol rings in an up position.

(i) Pseudorotation. The pseudorotation of the *winged* cone (Figure 2a) consists of one concerted process in which hydrogen bonds are broken nor formed. The transition state is a C_6 symmetric cone (Figure 3a). The energy of the transition state is only $3.1 \text{ kcal mol}^{-1}$ higher than the energy of the *winged* cone (Table 1). The electrostatic energy is $2.0 \text{ kcal mol}^{-1}$ lower, indicating that the hydrogen bond geometry is more favorable in the transition state than in the *winged* cone. The energy barrier is mainly composed of the higher dihedral angle energy ($+13.1 \text{ kcal mol}^{-1}$), but is lowered by the van der Waals energy ($-4.0 \text{ kcal mol}^{-1}$).

Pseudorotation of the *pinched* cone will always be accompanied with breaking of hydrogen bonds, because the exchanging methylene bridges have to pass either *through* the underlying hydrogen bond or *over* the

underlying hydrogen bond. In both cases, the adjacent aromatic rings are rotated with respect to each other, and the hydroxy-hydroxy distance is increased which breaks the hydrogen bond (Figure 4). Both pathways of methylene exchange have been calculated by providing the appropriate initial intermediates. Whatever the intermediate, all calculated pathways of pseudorotation of the *pinched* cone proceeded via the same methylene through the hydrogen bond pathway (Figure 2d). At first, two methylene moieties change from inside to outside positions (transition states at $\lambda = 0.9$ and 1.7 \AA , respectively). Subsequently, the reaction proceeds via a C_6 -like conformation ($\lambda = 3.6 \text{ \AA}$). Finally two other methylene moieties change from outside to inside positions via nearly identical transition states as the first two (transition states at $\lambda = 5.6$ and 6.5 \AA , respectively). The energy of the rate-limiting transition state at $\lambda = 4.1 \text{ \AA}$ is $19.4 \text{ kcal mol}^{-1}$, mainly due to an increase in electrostatic energy ($14.2 \text{ kcal mol}^{-1}$) and dihedral energy ($10.0 \text{ kcal mol}^{-1}$).

(ii) Inversion. The inversion of the *winged* cone is a stepwise process with six transition states for every methylene bridge exchanging from inside to outside positions. Multiple hydrogen bonds are broken during

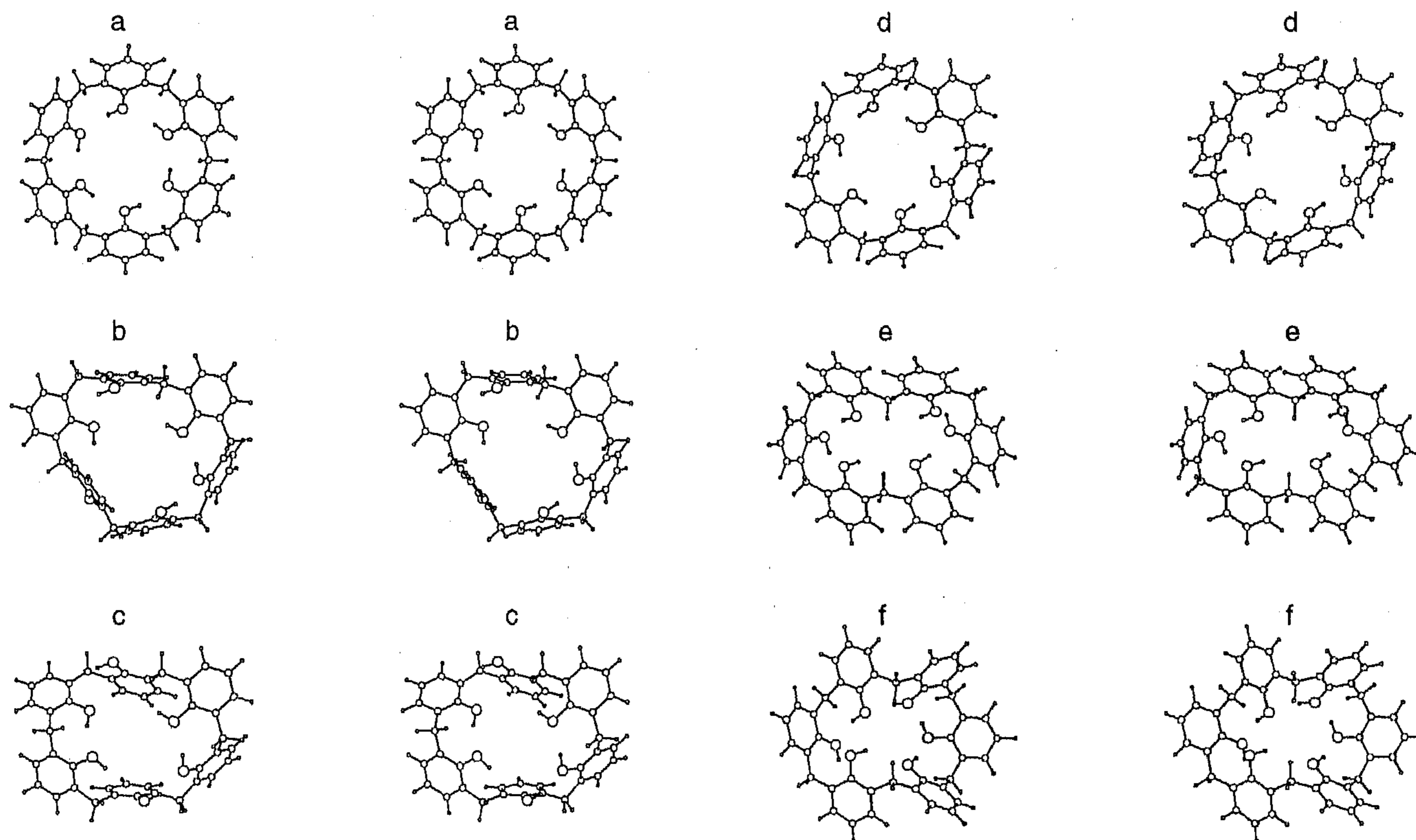


Figure 3. Rate-limiting transition state conformations of **3**. Depicted are pseudorotation (a), inversion (b), and pseudorotation/inversion (c) of the *winged* cone and pseudorotation (d), inversion (e), and pseudorotation/inversion (f) of the *pinched* cone.

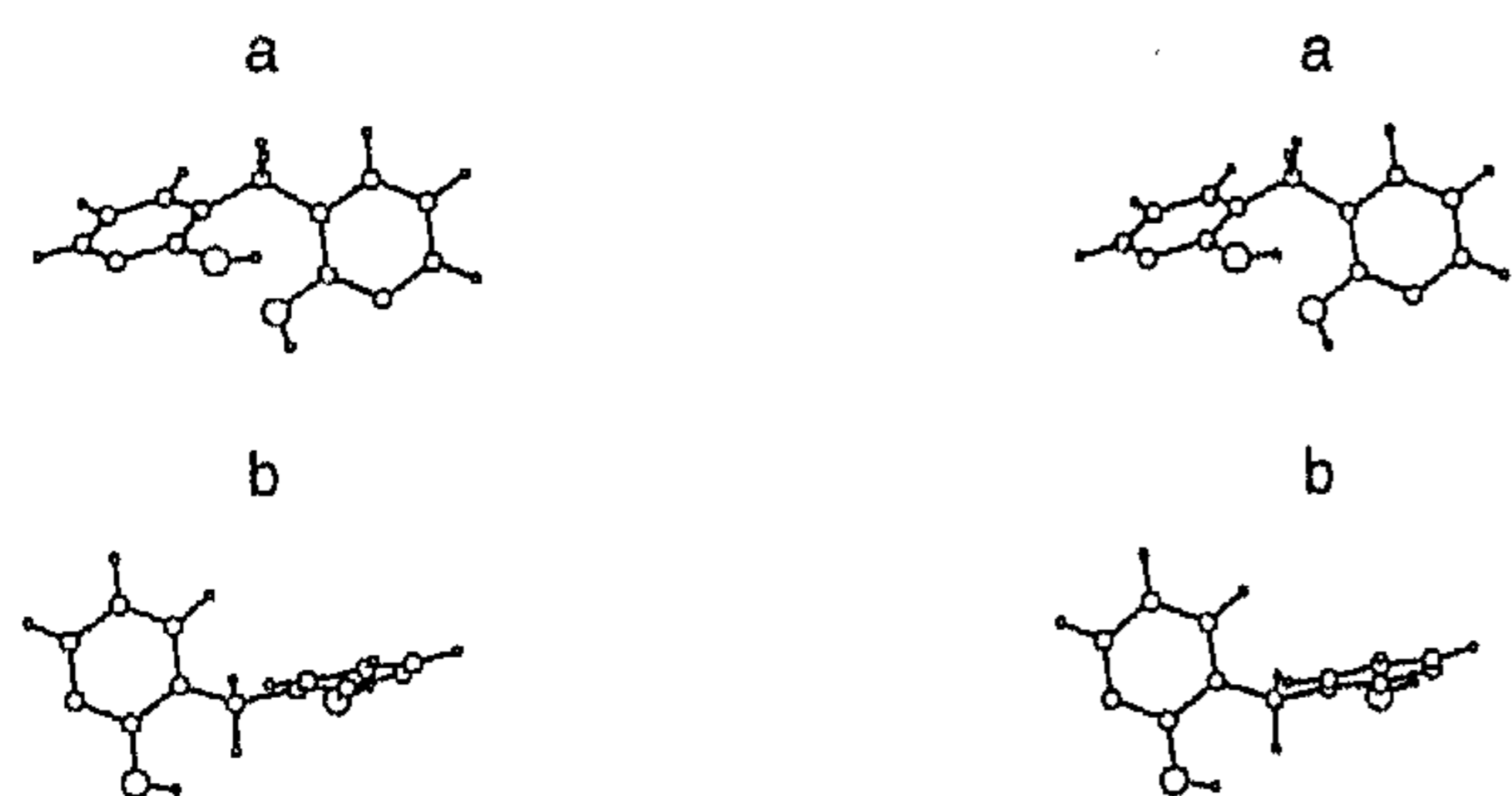


Figure 4. Two possible exchange pathways between inside/outside positions of the methylene bridges of the *pinched* cone of **3**. The methylene moiety can either move over (a) or through (b) the underlying hydrogen bond. The view is from inside the cavity. When the methylene bridge passes over the hydrogen bond, the aromatic ring on the left bends outside the cavity. When the methylene bridge passes through the hydrogen bond, the aromatic ring on the right bends inside the cavity. In either case the hydrogen bond will be broken.

the interconversion. The rate-limiting step is the fifth saddle point at $\lambda = 8.1$ Å with an energy barrier of 13.1 kcal mol⁻¹ with respect to the minimized *winged* cone. Along the reaction coordinate, four conformations are encountered that are lower in energy than the minimized *winged* cone (at $\lambda = 2.1, 4.5, 6.6,$ and 9.7 Å, respectively). The lowest minimum, at $\lambda = 9.7$ Å, is a *pinched* cone-like conformation with only one methylene bridge pointing inward (instead of two).

The inversion of the *pinched* cone also proceeds stepwise, via five saddle points. The energy barrier is 26.7 kcal mol⁻¹ with an electrostatic contribution of +25.2 kcal mol⁻¹, indicating the rupture of the hydrogen bonds in the rate-limiting transition state. First, two diametrical methylene bridges (3 and 6 in Figure 1a) pass one after the other over the hydrogen bonds to outside positions (at $\lambda = 1.0$ and 1.8 Å, respectively). Next, the two

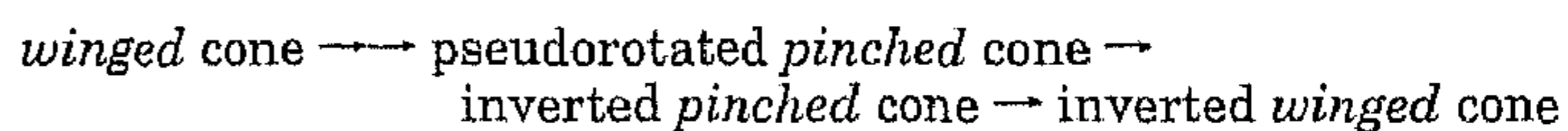
pinched methylene bridges pass consecutively through the hydrogen bonds ($\lambda = 4.3$ Å). Finally, the last two methylene bridges pass over the hydrogen bonds at $\lambda = 5.3$ and 6.2 Å, respectively.

(iii) Inversion Combined with Pseudorotation.

For the *pinched* cone, four methylene moieties have to exchange during pseudorotation, and six during inversion. When the processes of pseudorotation and inversion are combined, only two methylene moieties have to exchange between inside and outside positions. This cooperative effect is only possible for the *pinched* cone where the methylene exchanges are rate limiting.²³ The calculated combined inversion/pseudorotation process of the *pinched* cone has an energy barrier of 13.0 kcal mol⁻¹, which is indeed considerably lower than the energy barriers of either inversion or pseudorotation. In the rate-limiting step at $\lambda = 0.7$ Å, one aromatic ring adjacent to a *pinched* methylene bridge has rotated, which results in the breaking of two hydrogen bonds. At the other two saddle points, at $\lambda = 1.5$ and 2.3 Å, the methylene moieties pass one after the other through the hydrogen bonds. But for every hydrogen bond that is broken, one new hydrogen bond is simultaneously formed, so that during the whole process only two hydrogen bonds are broken at a time.

The TRAVEL calculations of **3** clearly show that for the *pinched* cone the combined pseudorotation/inversion process is by far favored over either pseudorotation or

(23) For the *winged* Cone, there is a possible cooperative effect of combining pseudorotation with inversion in the following process:



However, the rate-limiting step is now one of the *winged*/*pinched* cone exchanges (Figure 2c). The combined pseudorotation/inversion process of the *winged* cone showed no cooperativity, the pseudorotation and inversion proceeded separately (data not shown).

inversion alone. The energy of the transition state of this combined process is even lower than the energy of the minimized *winged* cone. For the *winged* cone, two interconversions proceed via conformations that are lower in energy than the *winged* cone itself (inversion and interconversion to the *pinched* cone). This demonstrates again the high energy of the *winged* cone with respect to the *pinched* cone. The reaction path calculations show that the combined pseudorotation/inversion of the *pinched* cone is the only process measurable at room temperature.²⁴ The TRAVEL calculations strongly support our view that the processes of pseudorotation and inversion observed by Molins *et al.* are one concerted process. The ΔG^\ddagger of inversion measured by Gutsche is only slightly dependent on solvent.⁴ We therefore expect that the entropy contribution to ΔG^\ddagger is small and that the calculated activation energy can be compared to the experimental ΔG^\ddagger . The calculated activation energy of 13.0 kcal mol⁻¹ compares favorably to the measured activation free energies⁶ for pseudorotation (12.2 kcal

mol⁻¹) and inversion (12.8 kcal mol⁻¹), which to our opinion are two independently measured activation free energies of the same process.

Conclusions

The *pinched* cone conformation of unsubstituted calix-[6]arene **3** is favored over the *winged* cone conformation by 16.2 kcal mol⁻¹ and is in better agreement with experimentally observed proton-proton distances. Reaction path calculations of both cone conformations show that the experimentally observed dynamic processes of pseudorotation and inversion are one concerted pseudorotation/inversion process of the *pinched* cone. The calculated activation energy for the concerted process of 13.0 kcal mol⁻¹ is in excellent agreement with the experimentally determined free energy barriers of 12.2 and 12.8 kcal mol⁻¹. Hexahydroxycalix[6]arenes adopt the *pinched* cone conformation in both the crystal state and in solution. The *winged* cone conformation proposed by Molins *et al.* is a local minimum on the energy surface, whereas the *pinched* cone is the global minimum.

(24) Apart from hydrogen bond reversal which has such a low energy barrier that it is only observable at low temperature (183 K).^{6,22}

JO960865O